Acta Pharmaceutica Sinica B 2015;5(1):67–73

HOSTED BY

Chinese Pharmaceutical Association
Institute of Materia Medica, Chinese Academy of Medical Sciences

Acta Pharmaceutica Sinica B

www.elsevier.com/locate/apsb
www.sciencedirect.com

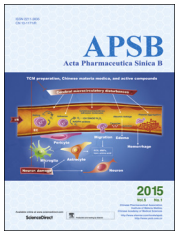

ORIGINAL ARTICLE

Design, synthesis and evaluation of genistein-polyamine conjugates as multi-functional anti-Alzheimer agents

Xin Zhang, Jiang Wang, Chen Hong, Wen Luo*, Chaojie Wang*

Key Laboratory of Natural Medicine and Immuno-Engineering, Henan University, Kaifeng 475004, China

Received 14 October 2014; received in revised form 27 November 2014; accepted 11 December 2014

KEY WORDS

Genistein;
Polyamine;
Alzheimer's disease;
Acetylcholinesterase;
Molecular modeling;
Metal-chelating;
Inhibition;
Rivastigmine

Abstract A series of genistein-polyamine conjugates (**4a–4h**) were designed, synthesized and evaluated as multi-functional anti-Alzheimer agents. The results showed that these compounds had significant cholinesterases (ChEs) inhibitory activity. Compound **4b** exhibited the strongest inhibition to acetylcholinesterase (AChE) with an IC_{50} value of 2.75 μmol/L, which was better than that of rivastigmine (5.60 μmol/L). Lineweaver–Burk plot and molecular modeling study showed that compound **4b** targeted both the catalytic active site (CAS) and the peripheral anionic site (PAS) of AChE. Besides, compound **4b** showed potent metal-chelating ability. In addition, it was found that **4a–4h** did not affect HepG-2 cell viability at the concentration of 10 μmol/L.

*Corresponding authors. Tel./fax: +86 371 22864665.
E-mail addresses: luowen83@163.com (Wen Luo), wcjsxq@163.com (Chaojie Wang).

Peer review under responsibility of Institute of Materia Medica, Chinese Academy of Medical Sciences and Chinese Pharmaceutical Association.

http://dx.doi.org/10.1016/j.apsb.2014.12.008

1. Introduction

Alzheimer's disease (AD), the most common form of neurodegenerative senile dementia, is associated with selective loss of cholinergic neurons and reduced level of acetylcholine neurotransmitter. It is characterized by memory deficit and progressive impairment of cognitive functions[1]. AD affects millions of elderly people, and the number of patients is expected to increase in the next 20 years. Many factors have been found to be implicated in AD, such as low levels of acetylcholine, β-amyloid deposits, oxidative damage and metal ions, which seem to play significant roles in the disease[2]. Current treatment of AD focuses on increasing cholinergic neurotransmission in the brain by inhibiting cholinesterases (ChEs) with medicines including tacrine, donepezil, rivastigmine and galantamine[3]. Unfortunately, the potential effectiveness offered by the above inhibitors is often limited by their side effects. For example, clinical studies have shown that tacrine has hepatotoxic liability[4]. Due to the multi-pathogenesis of AD, one of the current strategies is to develop novel anti-AD agents with multiple potencies[5].

Genistein is biosynthetically the simplest isoflavonoid compound of the Leguminosae[6]. It expresses a wide range of biological activities, such as antioxidant, anti-cancer and antimicrobial[7–9]. In recent years, it was reported that genistein showed neuroprotective effect and ameliorated learning and memory deficits in the AD rat model[10,11]. Besides, a number of genistein derivatives have been reported as anti-AD agents in the past years (Fig. 1)[12,13]. These results indicate that genistein could be used as leading compound for the treatment of AD.

Polyamines are aliphatic molecules with amine groups distributed along their structures[14]. They have always been the concern of medicinal chemists as a universal template[15]. Our group has been involved in the development of polyamine conjugates as potential drugs for many years[16–19]. It was found that quinoline-polyamine conjugates exhibited potent ChEs inhibition activity and polyamine occupied the gorge of AChE[20]. Therefore, in the present study, in order to enhance the pharmacological potential of genistein, a series of genistein conjugates modified with polyamine were designed, synthesized as anti-Alzheimer agents.

2. Results and discussion

2.1. Synthesis of target compounds *4a–4h*

The synthetic routes to target compounds are summarized in Scheme 1. The starting material genistein **1** was treated with ethyl 2-chloroacetate in acetone to give intermediate **2**, which was heated with K_2CO_3 in water and then mixed with HCl yielding compound **3**. Then compound **3** converted to the intermediates by reaction with amines or Boc protected polyamines in DMF. At last, the Boc groups subsequently were removed using HCl (4 mol/L) at room temperature, producing target compounds **4a–4h** as hydrochloride salts. All the structures of the target compounds were confirmed by ^{1}H NMR, ESI-MS and elemental analysis.

2.2. Enzyme inhibition assays

All the newly synthesized compounds (**4a–4h**) were screened against AChE and BChE *in vitro* according to the modified Ellman method. Rivastigmine was used as control. The ChEs inhibition results were listed as the inhibition ratio at a tested concentration of 50 μmol/L (Table 1). We also tested the IC_{50} value of compounds **4b** and **4h** (Table 2).

The results showed that all of the target compounds possessed ChEs inhibition activity, and compound **4b** exhibited the strongest inhibition to AChE with an IC_{50} value of 2.75 μmol/L which was better than rivastigmine (5.60 μmol/L), compound **4h** also showed good activity with IC_{50} values of 46.59 μmol/L. Genistein, the parent molecule, inhibited the AChE activity to less than 50% at the concentration of 100 μmol/L (Table 2). It indicated that conjugation polyamines with genistein could increase the inhibition activity of AChE. Besides, it seemed that AChE inhibitory potency of conjugates was closely related to the length and the end group of the polyamine chain. Compounds (**4b–4d**) modified by diamine were more active than compounds conjugated with monoamine or triamine.

In the assay of BChE inhibtion studies, compound **4h** showed the most potent inhibition for BChE with an inhibition rate of

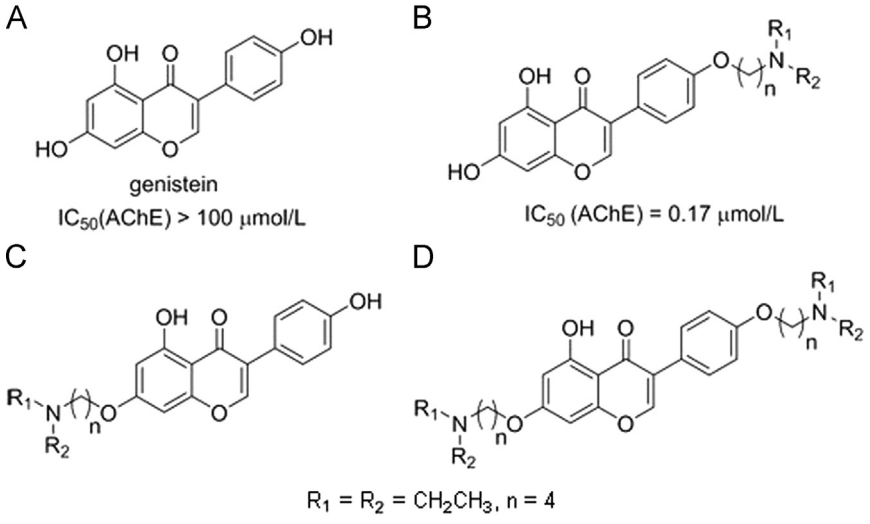

Figure 1 Chemical structures of genistein and genistein derivatives.

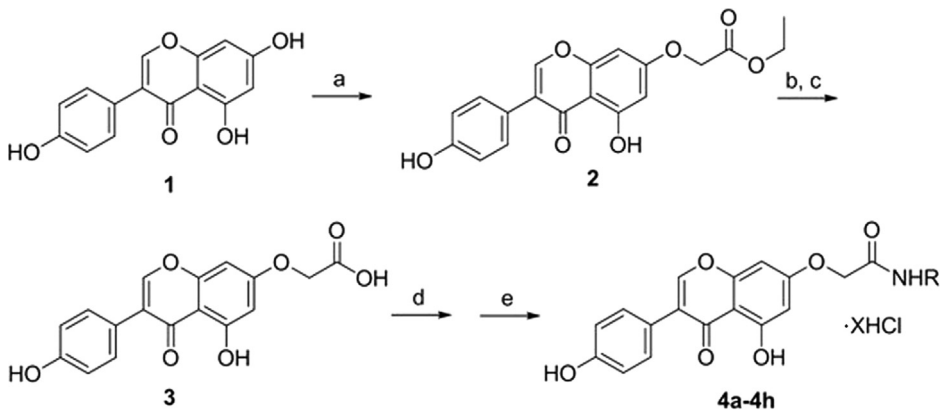

Scheme 1 Reaction conditions and reagents: (a) ethyl 2-chloroacetate, K_2CO_3, I_2, acetone, reflux, 6 h; (b) DMSO, K_2CO_3, H_2O, 85 °C, 10 h; (c) 10% HCl, rt, overnight; (d) EDC, NHS, amines, DMF, rt, overnight; (e) 4 mol/L HCl, EtOH, rt, overnight.

Table 1 Inhibitory activity of target compounds for AChE and BChE.

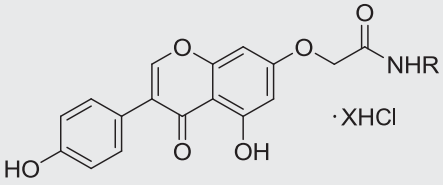

Compound	R	X	Inhibition ratios for AChE[a] (%)	Inhibition ratios for BChE[a] (%)
4a		0	7.88 ± 3.58	1.19 ± 0.59
4b		1	90.40 ± 1.23	26.05 ± 2.52
4c		1	37.02 ± 2.07	13.77 ± 1.05
4d	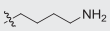	1	34.49 ± 2.76	9.02 ± 0.23
4e	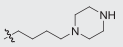	2	19.28 ± 1.87	11.72 ± 0.82
4f	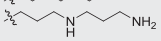	2	10.19 ± 0.44	9.52 ± 1.48
4g	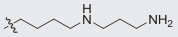	2	16.54 ± 1.36	17.88 ± 2.83
4h	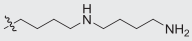	2	51.04 ± 0.55	39.20 ± 5.64
Rivastigmine	–	–	86.45 ± 0.71	94.60 ± 3.19

[a]Inhibition ratios for AChE and BChE in the presence of 50 μmol/L compound (mean ± SEM of two experiments), AChE from *Electric Eel*, BChE from equine serum.

39.20% at the concentration of 50 μmol/L. These compounds showed quite weaker inhibitory effect than AChE. The result indicated that these genistein derivatives might favor the binding to AChE, which was in agreement with the literature reported[12].

2.3. *Kinetic characterization of AChE inhibition*

The inhibition type of AChE was investigated by graphical analysis of steady state inhibition data (Fig. 2A) using compound **4b** as a typical example. The Lineweaver–Burk plots describing **4b** inhibition showed both increasing slopes and increasing intercepts with higher inhibitor concentration, indicating a mixed-type inhibition. These results revealed that compound **4b** bounded to both the catalytic active site (CAS) and the peripheral anionic site (PAS) of AChE, which is also in agreement with the results of our molecular modeling studies.

2.4. *Molecular modeling*

To investigate the interaction mode of compound **4b** with *Tc*AChE (protein data bank (PDB) code:1ZGB) molecular modeling was carried out by AUTODOCK 4.0 package with PyMOL program (Fig. 2B)[21,22]. The docking result demonstrated that compound **4b** exhibited multiple binding modes with AChE. In the **4b**-*Tc*AChE complex, compound **4b** occupied the entire enzymatic CAS, midgorge and PAS. The charged nitrogen made a cation–π interaction with the Trp84. At the midgorge recognition site, the chromone moiety displayed classic π–π stacking with the phenyl ring of Try334, with the ring-to-ring distance being 4.4 Å and 4.7 Å, respectively. At the PAS, the benzene of genistein moiety stacked against the Trp279 through π–π interaction with the distance of 4.4 Å. The result showed that compound **4b** was able to bind both CAS and PAS of AChE which was in agreement with the result of kinetic study.

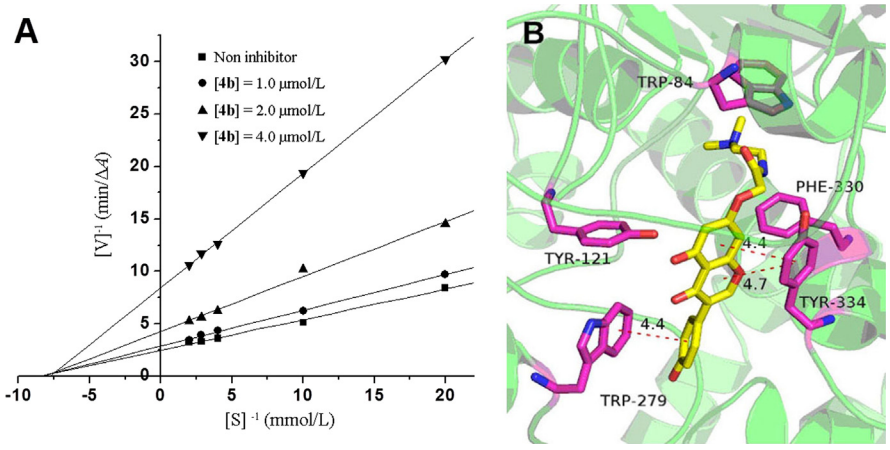

Figure 2 Lineweaver–Burk plots (A) and the docking model (B) for compound **4b** with *Tc*AChE.

Table 2 IC_{50} of some target compounds for AChE and BChE.

Compound	IC_{50} AChE[a] (μmol/L)	IC_{50} BChE[a] (μmol/L)
4b	2.75±0.28	>50
4h	46.59±3.87	>50
Genistein	>100	>100
Rivastigmine	5.60±1.50	1.65±0.05

[a]IC_{50} (μmol/L), 50% inhibitory concentration (mean±SEM of three experiments) of AChE or BChE.

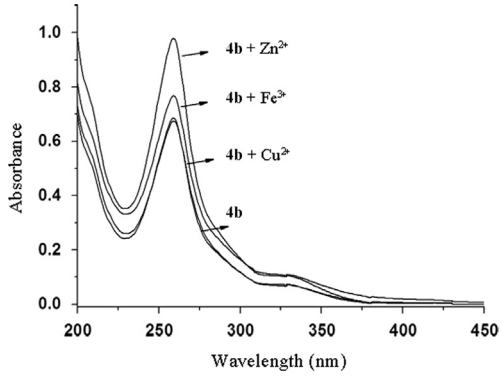

Figure 3 UV–Vis spectrum of compound **4b** (20 μmol/L) alone or in the presence of 20 μmol/L Fe^{3+}, Cu^{2+} and Zn^{2+}.

2.5. *Metal-chelating study*

The abnormally high levels of biometals in affected areas of the brain catalyze the formation of reactive oxygen species, which further aggravates oxidative stress contributing to β-amyloid formation. These effects have rendered metal chelators as very promising drugs for AD. Thus, the chelation abilities of compound **4b** towards biometal Fe^{3+}, Cu^{2+} and Zn^{2+} in water were studied by UV-Vis spectrometry. The results in Fig. 3 shows that the absorbance spectra of **4b** exhibited an apparent increase after the addition of Fe^{3+} or Zn^{2+}, and a red-shift in the maximum absorption from 259 nm to 268 nm occurred. This result indicated that there was an interaction between compound **4b** and Fe^{3+} or Zn^{2+} ion due to complex formation[24]. However, slight changes were observed in the UV spectrum of **4b** after adding Cu^{2+}, indicating the poor chelating ability of compound **4b** for Cu^{2+} ion.

Table 3 MTT assay of HepG-2 cell viability.

Compound	Inhibition ratios[a] (%)
4a	6.40
4b	1.53
4c	14.57
4d	1.17
4e	8.51
4f	11.74
4g	16.72
4h	16.30
Tacrine	57.35

[a]Inhibition ratios for HepG-2 cell viability in the presence of 10 μmol/L compound, each sample is the mean of three independent experiments.

2.6. *MTT assay of cell viability*

The toxicity of synthesized compounds was determined in HepG-2. Results indicated that the most potent two inhibitors, **4b** and **4h**, showed no obvious effect on cell viability at concentration of 10 μmol/L, as shown in Table 3. Compared with tacrine, they had lower toxicity on cell viability.

3. Conclusions

In conclusion, a series of novel genistein–polyamine conjugates (**4a–4h**) were designed, synthesized and evaluated for cholinesterase inhibition, metal-chelating activity and human hepatoma cell viability. Results indicated that these compounds had significant ChEs inhibitory activity. Compound **4b** exhibited the strongest inhibition to AChE with an IC_{50} value of 2.75 μmol/L. Lineweaver–Burk plot and molecular modeling study showed that compound **4b** targeted both the CAS and PAS of AChE. Besides, compound **4b** showed potent metal chelating ability. In addition, these compounds showed low cytotoxicity by MTT assay *in vitro*. Compound **4b** may be considered to be a novel multi-functional low-toxic drug candidate for the treatment of AD.

4. Experimental

4.1. Materials

Acetylcholinesterase (AChE, E.C. 3.1.1.7, from *Electric Eel*), butyrylcholinesterase (BChE, E.C. 3.1.1.8, from equine serum), 5,5′-dithiobis-(2-nitrobenzoic acid) (DTNB), butyrylthiocholine chloride (BTC), and acetylthiocholine chloride (ATC) were purchased from Sigma-Aldrich and rivastigmine hydrochloride standard was purchased from Sunve Pharmaceutical Co., Ltd. (Shanghai, China). ^{1}H NMR spectra were recorded using TMS as the internal standard in DMSO or D_2O with a Bruker AV-400 spectrometer at 400 MHz. MS spectra were recorded on a Shimadzu LCMS-2010A instrument with an ESI mass selective detector. Elemental analyses were performed on a Gmbe VarioEL Elemental Instrument. Flash column chromatography was performed with silica gel (200–300 mesh) purchased from Qingdao Haiyang Chemical Co., Ltd.

4.2. Chemistry

4.2.1. Synthesis of intermediate **2**

Genistein (2.70 g, 10 mmol), ethyl 2-chloroacetate (1.47 g, 12 mmol), anhydrous K_2CO_3 (0.69 g, 5 mmol) and catalytic amount KI (0.05 g) were added in anhydrous acetone (100 mL), and the mixture was refluxed for 6 h. The solution was filtered and the filter cake was recrystallized from EtOH to give light yellow solid 2.60 g; Yield 73%; MS (ESI) *m/z* 357.1 $[M+H]^+$.

4.2.2. Synthesis of intermediate **3**

Compound **2** (0.71 g, 2 mmol), 5% Na_2CO_3 and DMSO (40 mL) were heated at 85 °C for 10 h. Then the reaction mixture was poured into 10% HCl (300 mL), kept overnight and filtered. The filter cake was recrystallized from EtOH to give light brown solid 0.46 g; Yield 70%.

4.2.3. Synthesis of target compounds ***4a–4h***

Compound **3** (0.36 g, 1 mmol), 1-[3-(dimethylamino)propyl]-3-ethylcarbodiimide (EDC, 0.29 g, 1.5 mmol) and *N*-hydroxysuccinimide (NHS, 0.17 g, 1.5 mmol) were stirred at room temperature for 1.5 h, and then amines or Boc protected amines (1.2 mmol) were added. The mixture was stirred at room temperature overnight. Then the solvent was poured into water and extracted with ethyl acetate (20 mL × 3). The solution was dried over anhydrous Na_2SO_4 and concentrated. The intermediates were purified by flash chromatography with chloroform/methanol/ammonia (20:1:0.5, *v/v/v*) elution.

The intermediates were dissolved in EtOH (10 mL) and stirred at 0 °C for 10 min. Then 4 mol/L HCl (diluted with EtOH) was added dropwise at 0 °C. The reaction mixture was stirred at room temperature overnight. The solution typically gave a white solid precipitate. The precipitate was collected and washed several times with absolute ethanol and ether, and dried under vacuum to give pure target compounds **4a–4h**.

N-butyl-2-(5-hydroxy-3-(4-hydroxyphenyl)-4-oxo-4H-chromen-7-yloxy)acetamide (***4a***): White solid; m.p. 180–183 °C; Yield 63%. ^{1}H NMR (400 MHz, DMSO-d_6): δ 12.95 (s, 1H), 9.63 (s, 1H), 8.43 (s, 1H), 8.16 (s, 1H), 7.44–7.36 (m, 2H), 6.87–6.79 (m, 2H), 6.66 (d, J=2.3 Hz, 1H), 6.45 (d, J=2.3 Hz, 1H), 4.61 (s, 2H), 3.13 (dd, 2H, J=13.0, 6.8 Hz), 1.46–1.37 (m, 2H), 1.26 (dd, J=15.1, 7.5 Hz), 0.86 (t, J=7.3 Hz). ESI-MS *m/z*: 384.4 $[M+H]^+$. Anal. Calcd. for $C_{21}H_{21}NO_6 \cdot 0.1C_2H_5OH$: C, 65.52; H, 5.76; N, 3.60, Found C, 65.44; H, 5.82; N, 3.43.

N-(2-(dimethylamino)ethyl)-2-(5-hydroxy-3-(4-hydroxyphenyl)-4-oxo-4H-chromen-7-yloxy)acetamide hydrochloride (***4b***): White solid; m.p. 143–145 °C; Yield 49%. ^{1}H NMR (400 MHz, D_2O): δ 7.99–7.89 (m, 1H), 7.22 (s, 2H), 6.81 (s, 2H), 6.41–6.34 (m, 1H), 6.22 (s, 1H), 4.36 (s, 2H), 3.52 (s, 2H), 3.19 (s, 2H), 2.58 (s, 6H). ESI-MS *m/z*: 399.4 $[M+H\text{-}HCl]^+$. Anal. Calcd. for $C_{21}H_{21}N_2O_6 \cdot HCl \cdot 0.4H_2O$: C, 57.05; H, 5.43; N, 6.34, Found C, 57.03; H, 5.52; N, 6.73.

N-(3-aminopropyl)-2-(5-hydroxy-3-(4-hydroxyphenyl)-4-oxo-4H-chromen-7-yloxy)acetamide hydrochloride (***4c***): White solid; m.p. 187–189 °C; Yield 50%. ^{1}H NMR (400 MHz, D_2O): δ 7.98 (s, 1H), 7.27 (d, 2H, J=8.5 Hz), 6.87 (d, 2H, J=8.4 Hz), 6.38 (s, 1H), 6.23 (d, 1H, J=2.0 Hz), 4.31 (s, 2H), 3.30 (t, 2H, J=6.8 Hz), 3.00–2.93 (m, 2H), 1.90–1.82 (m, 2H). ESI-MS *m/z*: 385.4 $[M+H\text{-}HCl]^+$. Anal. Calcd. for $C_{20}H_{20}N_2O_6 \cdot HCl \cdot 3.5H_2O$: C, 49.64; H, 5.83; N, 5.79, Found C, 49.69; H, 5.60; N, 5.58.

N-(4-aminobutyl)-2-(5-hydroxy-3-(4-hydroxyphenyl)-4-oxo-4H-chromen-7-yloxy)acetamide hydrochloride (***4d***): White solid; m.p. 214–216 °C; Yield 48%: ^{1}H NMR (400 MHz, D_2O): δ 7.83 (s, 1H), 7.14 (s, 2H), 6.76 (d, 2H, J=7.9 Hz), 6.21 (s, 1H), 6.08 (s, 1H), 4.14 (s, 2H), 3.12 (t, 2H, J=6.8 Hz), 2.95–2.85 (m, 2H), 1.50 (dd, 4H, J=31.9, 7.1 Hz). ESI-MS *m/z*: 399.4 $[M+H\text{-}HCl]^+$. Anal. Calcd. for $C_{21}H_{22}N_2O_6 \cdot HCl \cdot 2.5H_2O$: C, 52.56; H, 5.88; N, 5.84, Found C, 52.64; H, 5.51; N, 5.57.

2-(5-hydroxy-3-(4-hydroxyphenyl)-4-oxo-4H-chromen-7-yloxy)-N-(4-(piperazin-1-yl)butyl)acetamide hydrochloride (***4e***): White solid; m.p. 215–217 °C; Yield 46%: ^{1}H NMR (400 MHz, D_2O): δ 7.95 (s, 1H), 7.23 (d, 2H, J=8.4 Hz), 6.81 (d, 2H, J=8.5 Hz), 6.36 (s, 1H), 6.19 (s, 1H), 4.30 (s, 2H), 3.47 (s, 8H), 3.14 (dd, 4H, J=14.9, 7.6 Hz), 1.62 (s, 2H), 1.50–1.40 (m, 2H). ESI-MS *m/z*: 468.5 $[M+H\text{-}2HCl]^+$. Anal. Calcd. for $C_{25}H_{29}N_3O_6 \cdot 2HCl \cdot 0.4H_2O$: C, 54.83; H, 5.85; N, 7.67, Found C, 54.49; H, 5.78; N, 7.63.

N-(3-(3-aminopropylamino)propyl)-2-(5-hydroxy-3-(4-hydroxyphenyl)-4-oxo-4H-chromen-7-yloxy)acetamide hydrochloride (***4f***): White solid; m.p. 147–149 °C; Yield 37%: ^{1}H NMR (400 MHz, D_2O): δ 7.96 (s, 1H), 7.24 (d, 2H, J=7.8 Hz), 6.82 (d, 2H, J=8.0 Hz), 6.37 (s, 1H), 6.20 (s, 1H), 4.31 (s, 2H), 3.24 (t, 2H, J=6.6 Hz), 3.06–2.92 (m, 6H), 1.97 (dt, J=15.8, 7.9 Hz), 1.86–1.77 (m, 2H). ESI-MS *m/z*: 442.5 $[M+H\text{-}2HCl]^+$. Anal. Calcd. for $C_{23}H_{27}N_3O_6 \cdot 2HCl \cdot 1.2H_2O$: C, 51.54; H, 5.90; N, 7.84, Found C, 51.86; H, 5.92; N, 7.45.

N-(4-(3-aminopropylamino)butyl)-2-(5-hydroxy-3-(4-hydroxyphenyl)-4-oxo-4H-chromen-7-yloxy)acetamide hydrochloride (***4g***): QWhite solid; m.p. 176–178 °C; Yield 35%: ^{1}H NMR (400 MHz, D_2O): δ 7.86 (s, 1H), 7.15 (d, 2H, J=8.6 Hz), 6.74 (d, 2H, J=8.6 Hz), 6.23 (d, 1H, J=2.0 Hz), 6.08 (d, 1H, J=2.2 Hz,), 4.13 (s, 2H), 3.08 (t, 2H, J=6.9 Hz), 3.01–2.90 (m, 6H), 1.92 (dd, 2H, J=10.5, 5.3 Hz), 1.52 (d, 2H, J=6.3 Hz), 1.45–1.37 (m, 2H). ESI-MS *m/z*: 456.5 $[M+H\text{-}2HCl]^+$. Anal. Calcd. for $C_{24}H_{29}N_3O_6 \cdot 2HCl \cdot 4H_2O$: C, 48.00; H, 6.55; N, 7.00, Found C, 48.01; H, 6.81; N, 7.38.

N-(4-(4-aminobutylamino)butyl)-2-(5-hydroxy-3-(4-hydroxyphenyl)-4-oxo-4H-chromen-7-yloxy)acetamide hydrochloride (***4h***): White solid; m.p. 187–189 °C; Yield 37%: ^{1}H NMR (400 MHz, D_2O): δ 7.62 (s, 1H), 7.04 (d, 2H), 6.71 (d, 2H, J=7.8 Hz), 5.97 (s, 2H), 3.98 (s, 2H), 3.13 (s, 2H), 3.04–2.95 (m, 6H), 1.72 (s, 4H), 1.63 (s, 2H), 1.49 (d, 2H, J=7.0 Hz). ESI-MS *m/z*: 470.5 $[M+H\text{-}2HCl]^+$. Anal. Calcd. for $C_{25}H_{31}N_3O_6 \cdot 2HCl \cdot 2.5H_2O$: C, 51.11; H, 6.52; N, 7.15, Found C, 51.03; H, 6.29; N, 6.93.

4.3. Enzyme inhibition assays

All the assays were under 0.1 mol/L KH_2PO_4/K_2HPO_4 buffer, pH 8.0, using a Shimadzu 2450 Spectrophotometer. Enzyme solutions were prepared to give 2.0 units/mL in 2 mL aliquots. The assay medium contained phosphate buffer (pH 8.0), 50 μL of 0.01 mol/L DTNB, 10 μL of enzyme, and 50 μL of 0.01 mol/L substrate (ATC). The substrate was added to the assay medium which contained enzyme, buffer and DTNB with inhibitor (0, 5, 10, 20, 35, and 50 μmol/L) after 15 min of incubation time. The activity was determined by measuring the increase in absorbance at 412 nm at 1 min intervals at 37 °C. Calculations were performed according to the method of the equation in Ellman et al.[23]. The *in vitro* BChE assay used the similar method described above. The concentration of compound that effected 50% inhibition of ChEs activities (IC_{50}) was calculated by nonlinear regression of the inhibition ratio–concentration curve, using Origin 7.5 program.

4.4. Kinetic characterization of AChE inhibition

Kinetic characterization of AChE was performed using a reported method. Six different concentrations of substrate were mixed in the 1 mL 0.1 mol/L KH_2PO_4/K_2HPO_4 buffer (pH 8.0), containing 50 μL of DTNB, 10 μL AChE and 50 μL substrate. Test compound was added into the assay solution and pre-incubated with the enzyme at 37 °C for 15 min, followed by the addition of substrate. Kinetic characterization of the hydrolysis of ATC catalyzed by AChE was done spectrometrically at 412 nm. A parallel control with no inhibitor in the mixture, allowed adjusting activities to be measured at various times.

4.5. Molecular modeling

The crystal structure of the torpedo AChE (code ID: 1ZGB) was obtained in the PDB after eliminating the inhibitor and water molecules. The 3D structure of compound **4b** was prepared as similar as previously described[20].

Docking studies were carried out using the AUTODOCK 4.0 program using ADT. The enzyme structure was used as an input for the AUTOGRID program. AUTOGRID performed a precalculated atomic affinity grid maps for each atom type in the ligand plus an electrostatics map and a separate desolvation map present in the substrate molecule. All maps were calculated with 0.375 Å spacing between grid points. The center of the grid box was placed at the bottom of the active site gorge (AChE [2.781 64.383 67.971]). The dimensions of the active site box were set at 50 Å × 46 Å × 46 Å.

Flexible ligand docking was performed for the compounds. Docking calculations were carried out using the Lamarckian genetic algorithm (LGA) and all parameters were the same for each docking.

4.6. Metal-chelating study

The chelating studies were made in water using a UV-Vis spectrophotometer (SHIMADZC UV-2450PC). The absorption spectrum of compound **4b** (20 μmol/L), alone or in the presence of $FeCl_3$, $CuSO_4$ or $ZnCl_2$ (20 μmol/L), was recorded with wavelength ranging from 200 to 500 nm after incubating for 30 min at room temperature. The final volume of reaction mixture was 1 mL, and the final concentrations of tested compound and metals were 20 μmol/L.

4.7. MTT assay of HepG-2 cell viability

Cells were cultured at 37 °C under a 5% CO_2 atmosphere. The antiproliferative ability of compounds was evaluated in HepG-2 cells by the conversion of MTT to a purple formazan precipitate as previously described[19]. Cells were seeded into 96-well plates at 5×10^3 cells/well. After 12 h, 10 μmol/L of compounds was subsequently added and incubated for 48 h. The inhibition rate was calculated from plotted results using untreated cells as 100%.

Acknowledgments

We thank the National Natural Science Foundation of China (Nos. 21172053 and 21302041), the China Postdoctoral Science Foundation (No. 2012M521391), the Postdoctoral Science Foundation of Henan Province (No. 2011015) and the Foundation of Henan Educational Committee (No. 14A350008) for financial support of this study.

Appendix A. Supporting information

Supplementary data associated with this article can be found in the online version at http://dx.doi.org/10.1016/j.apsb.2014.12.008.

References

1. Bartus RT, Dean RL, Beer B, Lippa AS. The cholinergic hypothesis of geriatric memory dysfunction. *Science* 1982;**217**:408–14.
2. Fernández-Bachiller MI, Pérez C, Campillo NE, Páez JA, González-Muñoz GC, Usán P, et al. Tacrine–melatonin hybrids as multifunctional agents for Alzheimer's disease, with cholinergic, antioxidant, and neuroprotective properties. *Chem Med Chem* 2009;**4**:828–41.
3. Rizzo S, Rivière C, Piazzi L, Bisi A, Gobbi S, Bartolini M, et al. Benzofuran-based hybrid compounds for the inhibition of cholinesterase activity, β amyloid aggregation, and Aβ neurotoxicity. *J Med Chem* 2008;**51**:2883–6.
4. Watkins PB, Zimmerman HJ, Knapp MJ, Garcon SI, Lewis KW. Hepatotoxic effects of tacrine administration in patients with Alzheimer's disease. *J Am Med Assoc* 1994;**271**:992–8.
5. Cavalli A, Bolognesi ML, Minarini A, Rosini M, Tumiatti V, Recanatini M, et al. Multi-target-directed ligands to combat neurodegenerative diseases. *J Med Chem* 2008;**51**:347–72.
6. Kaufman PB, Duke JA, Brielmann H, Boik J, Hoyt JE. A comparative survey of leguminous plants as sources of the isoflavones, genistein and daidzein: implications for human nutrition and health. *J Altern Complement Med* 1997;**3**:7–12.
7. Record IR, Dreosti IE, McInerney JK. The antioxidant activity of genistein *in vitro*. *J Nutr Biochem* 1995;**6**:481–5.
8. Ravindranath MH, Muthugounder S, Presser N, Viswanathan S. Anticancer therapeutic potential of soy isoflavone, genistein. *Adv Exp Med Biol* 2004;**546**:121–65.
9. Zhang LN, Cao P, Tan SH, Gu W, Shi L, Zhu HL. Synthesis and antimicrobial activities of 7-*O*-modified genistein derivatives. *Eur J Med Chem* 2008;**43**:1543–51.
10. Bang OY, Hong HS, Kim DH, Kim H, Boo JH, Huh K, et al. Neuroprotective effect of genistein against beta amyloid-induced neurotoxicity. *Neurobiol Dis* 2004;**16**:21–8.
11. Bagheri M, Joghataei MT, Mohseni S, Roghani M. Genistein ameliorates learning and memory deficits in amyloid β(1–40) rat model of Alzheimer's disease. *Neurobiol Learn Mem* 2011;**95**:270–6.

12. Shi DH, Yan ZQ, Zhang LN, Wang YR, Jiang CP, Wu JH. A novel 7-*O*-modified genistein derivative with acetylcholinesterase inhibitory effect, estrogenic activity and neuroprotective effect. *Arch Pharm Res* 2012;**35**:1645–54.
13. Qiang X, Sang Z, Yuan W, Li Y, Liu Q, Bai P, et al. Design, synthesis and evaluation of genistein-*O*-alkylbenzylamines as potential multi-functional agents for the treatment of Alzheimer's disease. *Eur J Med Chem* 2014;**76**:314–31.
14. Papadopoulou MV, Rosenzweig HS, Bloomer WD. Synthesis of a novel nitroimidazole-spermidine derivative as a tumor-targeted hypoxia-selective cytotoxin. *Bioorg Med Chem Lett* 2004;**14**:1519–22.
15. Tumiatti V, Milelli A, Minarini A, Rosini M, Bolognesi ML, Micco M, et al. Structure-activity relationships of acetylcholinesterase noncovalent inhibitors based on a polyamine backbone. 4. Further investigation on the inner spacer. *J Med Chem* 2008;**51**:7308–12.
16. Tian ZY, Xie SQ, Mei ZH, Zhao J, Gao WY, Wang CJ. Conjugation of substituted naphthalimides to polyamines as cytotoxic agents targeting the Akt/mTOR signal pathway. *Org Biomol Chem* 2009;**7**:4651–60.
17. Xie SQ, Wang JH, Ma HX, Cheng PF, Zhao J, Wang CJ. Polyamine transporter recognization and antitumor effects of anthracenymethyl homospermidine. *Toxicology* 2009;**263**:127–33.
18. Wang JH, Chen ZY, Xie SQ, Zhao J, Wang CJ. Synthesis and bioevaluation of aryl-guanidino polyamine conjugates targeting the polyamine transporter. *Bioorg Med Chem Lett* 2010;**20**:6421–5.
19. Wang YX, Zhang XB, Zhao J, Xie SQ, Wang CJ. Nonhematotoxic naphthalene diimide modified by polyamine: synthesis and biological evaluation. *J Med Chem* 2012;**55**:3502–12.
20. Luo W, Huang K, Zhang Z, Hong C, Wang CJ. Design, synthesis and cholinesterase inhibitory activity of quinoline-polyamine conjugates. *Acta Pharm Sin* 2013;**48**:269–75.
21. Morris GM, Goodsell DS, Halliday RS, Huey R, Hart WE, Belew RK, et al. Automated docking using a Lamarckian genetic algorithm and an empirical binding free energy function. *J Comput Chem* 1998;**19**:1639–62.
22. The PyMOL molecular graphics system. San Carlos, CA: DeLano Scientific; 2002. Available from: ⟨http://www.pymol.org/⟩.
23. Ellman GL, Courtney KD, Andres Jr. V, Feather-stone RM. A new and rapid colorimetric determination of acetylcholinesterase activity. *Biochem Pharmacol* 1961;**7**:88–95.
24. Bolognesi ML, Cavalli A, Valgimigli L, Bartolini M, Rosini M, Andrisano V, et al. Multi-target-directed drug design strategy: from a dual binding site acetylcholinesterase inhibitor to a trifunctional compound against Alzheimer's disease. *J Med Chem* 2007;**50**:6446–9.